A purely elastic self sustaining process in plane couette flow

T. W. Searle[1] and A. N. Morozov[1]†,

[1]SUPA, School of Physics and Astronomy, University of Edinburgh, Mayfield Road, Edinburgh, EH9 3JZ, UK

(Received ?; revised ?; accepted ?. - To be entered by editorial office)

Abstract goes here. Abstract goes here. Viscoelastic Kelvin-Helmholtz instability.

Key words: Authors should not enter keywords on the manuscript, as these must be chosen by the author during the online submission process and will then be added during the typesetting process (see http://journals.cambridge.org/data/relatedlink/jfm-keywords.pdf for the full list)

1. Introduction

We present a study of a purely elastic analogue of the Newtonian self-sustaining process presented in Waleffe (1997).

In 1997 Waleffe published a seminal article that demonstrated the existence of an exact coherent state that sustains turbulence in Newtonian plane Couette fluid flow. This solution consists of a self-sustaining process (SSP) of three phases. First the lift-up mechanism (sometimes called shear tilting), first studied by Ellingsen & Palm (1975); Landahl (1980). induced by streamwise rolls moves fluid between the plates. Due to conservation of momentum, this creates spanwise streaks in the streamwise velocity. In the second phase, these streaks become wavy in the streamwise direction. This is due to a linear instability in the streaky profile from a Kelvin-Helmholtz like effect as the streaks shear with the rest of the fluid. Finally, the nonlinear self-interaction terms from the wavy disturbance regenerate the original streamwise rolls.

This mechanism has proven very important. Since then, similar structures have been found in Newtonian pipe flow (both in numerical simulations in Wedin & Kerswell (2004) and in experiments in Hof *et al.* (2004)). The success of these exact solutions has fuelled the move towards an understanding of Newtonian turbulence in terms of these exact solutions, with the turbulent attactor constructed out of many exact solutions which become more densely packed as the Reynold's number increases. More recently, recurrent solutions have been discovered which give statistics which closely match those of experimental turbulent flows (Initially in Kawahara & Kida (2001), with others discovered in pipe flows in Kreilos & Eckhardt (2012) and two dimensional Kolmogorov flow by Chandler & Kerswell (2013)). According to the emerging picture, a turbulent fluid trajectory in phase space 'pinballs' between these states, spending most of its time very close to one of these solutions (see e.g. Cvitanović (2013)).

In 1990 Larson, Shaqfeh and Muller provided theoretical and experimental evidence of purely elastic instability Larson *et al.* (1990). Later, Byars *et al.* (1994) and Groisman &

† Email address for correspondence: T.W.Searle@sms.ed.ac.uk

Steinberg (2000) found spiral patterns and then full turbulence in a low Reynold's number plate-plate flow. The mechanism behind this instability is similar to the Weissenberg effect first observed by Karl Weissenberg (1947). These instabilities are part of a body of evidence which supports the existence of a different kind of turbulence, purely elastic turbulence, where the instabilities are generated and sustained by this Normal stress mechanism. Curved streamlines in the fluid lead to large normal stresses, which create more curved streamlines. It is this feedback which it is supposed will lead to a state of continuous instability. We think that this mechanism might provide a viscoelastic analogue of the Newtonian SSP.

Studies have already been carried out on a viscoelastic self-sustaining process (Stone *et al.* (2004, 2002); Sureshkumar *et al.* (1997)). However, these studies were concerned with high Reynold's number viscoelastic flows. Primarly they were interested in discovering how a small concentration of polymeric fluid can bring about a reduction in viscous drag in a fluid. They sought to explain this viscoelastic drag reduction by an appeal to the effect of the polymers on Waleffe's Newtonian self-sustaining process. These studies found that there is a minimum Reynold's number below which the SSP solution ceases to exist. We are find results which are consistent with this, however, the streak instabilty reappears at much lower Reynold's number, in the purely elastic regime. Neither the simulations in Sureshkumar *et al.* (1997) nor in Stone *et al.* (2004) give any results for $Re \sim 1$. They also introduce an unphysical approximation to the equations via a stress diffusion term. It is possible that in the purely elastic limit this stress diffusion will remove the large stress gradients necessary for instability.

The above studies find that the addition of a small amount of viscoelastic fluid serves to reduce the strength of the Newtonian exact coherent structures. The mechanism responsible for the effect of the polymeric fluid on the SSP is that of vortex unwinding. The polymeric stress opposes the nonlinearities that produce the vortices in the third phase of the process. In our study, the polymeric stresses can provide nonlinear terms for the production of vortices at very low Reynold's number, but they do so via the nonlinearities in the Oldroyd-B equation rather than the Navier-Stokes equation.

We expect chaotic systems to be structured by exact solutions to the equations. Given the above results, it seems that these exact solutions cannot be found by continuation from their counterparts for Newtonian flows. Instead, we have attempted to construct a viscoelastic analogue of the SSP as a means to constructing purely elastic exact coherent structures. The presence of these exact coherent structures is strongly suggested by earlier experimental (Pan *et al.* (2013); Samanta *et al.* (2013)) and numerical results (Morozov & van Saarloos (2007)?).

We use the Oldroyd-B model for the constituitive equation for the polymeric component of the fluid and the full Navier-Stokes equations,

$$Re\left[\frac{d\mathbf{v}}{dt} + \mathbf{v}\cdot\nabla\mathbf{v}\right] = -\nabla p + \beta\nabla^2\mathbf{v} + (1-\beta)\nabla\cdot\tau \tag{1.1}$$

$$\nabla\cdot\mathbf{v} = 0 \tag{1.2}$$

$$\tau + Wi\left[\frac{\partial\tau}{\partial t} + \mathbf{v}\cdot\nabla\tau - (\nabla v)^T\tau - \tau(\nabla v)\right] = (\nabla\mathbf{v})^T + \nabla\mathbf{v} \tag{1.3}$$

$$\tag{1.4}$$

where Re is the Reynold's number, Wi is the Weissenberg number, ∇ is the gradient operator, ∇^2 is the Laplacian and $\overset{\nabla}{\tau}$ is the upper convected derivative of the stress tensor. By direct numerical simulation, we investigate the three phases of the process.

First we use a Newton-Raphson method to show that streaky flow is a solution at low Re to the these equations when forced by streamwise independent rolls. Then we do a linear stability analysis of the streaky flow to show that these streaks are unstable to perturbations both dependent and independent of the streamwise wavenumber k_x. Finally we investigate how the eigenvectors which correspond to these instabilities will affect the base flow, completing the SSP.

At this point it is important to note that we are using one of the simplest models of a viscoelastic fluid, the Oldroyd-B fluid. They include all of the ingredients for the normal stress effect believed to be responsible for viscoelastic turbulence. However, it does not capture the shear thinning behaviour. It is also well known that under extensional flows (when $\lambda\dot{\epsilon} > 1/2$) the Oldroyd-B model breaks down. In the self-sustaining process as we have outlined it, there ought to be no extensional flows, so this danger turns out to be irrelevent (is this actually true?). Support for this point of view can be found in Stone Stone *et al.* (2004) where they find that in their simulations the polymer extension never exceeds 10% of the contour length.

The viscoelastic streamwise vortex forcing system we use here does produce streaks and these streaks do become unstable. The instabilities we observe can be wavy in the streamwise direction, but tend to have very long wavelengths. The instability that we observe is enough to produce feedback on the original rolls of the correct sign and symmetry. The instability can only be tracked for free slip boundary conditions, suggesting that the presence or otherwise of polymer slip at the walls might be important in this system.

2. Streaky profile

For the first step of the self-sustaining process we need to form a streaky base profile in the velocity. One way of forming these streaks is to start with large fluctuations in the wall-normal stress, τ_{yy}. This stress is then advected by the mean shear to give fluctuations in the stress in the streamwise direction and therefore a streaky base profile. An alternative is to use streamwise independent rolls and their associated pressure gradient. Similar to Waleffe Waleffe (1997), this gives,

$$Re\left[V(y,z)\frac{\partial U}{\partial y} + W(y,z)\frac{\partial U}{\partial z}\right] = \beta\nabla_2^2 U + (1-\beta)\left(\frac{\partial T_{xy}}{\partial y} + \frac{\partial T_{xz}}{\partial z}\right) \tag{2.1}$$

We use a Chebyshev-Fourier decomposition, with Chebyshev polynomials in the wall-normal (y) direction and Fourier modes in the spanwise (z) direction. We then solve for the streamwise velocity and Stresses of the base profile using equation 2.1 and the Oldroyd-B equation via a Newton-Raphson method. In order to decompose the system onto the computational grid, we take a Fourier and Chebyshev transform of the variables,

$$\check{G}(y,z) = \sum_{n=-N}^{N}\sum_{m=0}^{M-1} G_{m,n}\mathrm{e}^{in\gamma z}T_m(y) \tag{2.2}$$

where g stands for any of the base profile variables $(U, V, W, \boldsymbol{\tau}_{ij})$ in the problem and $T_m(y)$ is the mth Chebyshev polynomial of the first kind.

The system is driven by the standard no-slip boundary conditions on the streamwise velocity at the walls,

$$U(\pm 1) = 1 \tag{2.3}$$

and forcing terms introduced via fixing of the wall-normal and spanwise base profile

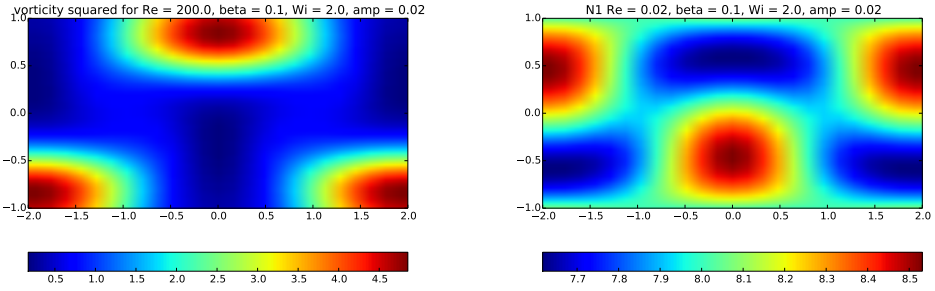

Figure 1: a) The magnitude of the vorticity of the fluid at $Re = 200$, $Wi = 2.0$, amp=0.02. b) The first normal stress difference in the polymeric fluid at $Re = 0.02$, $Wi = 2$, amp=0.02. The Newtonian vorticity and purely elastic first normal stress difference have large gradients in similar regions. However, the first normal stress difference also shows large gradients next to the wall.

velocities,

$$V(y,z) = V_0 \hat{v}(y) cos(\gamma z) \tag{2.4}$$

$$W(y,z) = -\frac{V_0}{\gamma}\frac{\partial \hat{v}}{\partial y}\sin(\gamma z) \tag{2.5}$$

Where,

$$\hat{v}(y) = \frac{\cos(py)}{\cos(p)} - \frac{\cosh(\gamma y)}{cosh(\gamma)} \tag{2.6}$$

p is given by solutions to $p\tan p + \gamma \tanh \gamma = 0$ and controls the number of rolls in the wall-normal direction. These velocities are a guess for the rolls derived from the lowest order eigenmode of the operator ∇^4, precisely the same rolls used in Waleffe (1997). This provides us with the streaky profile shown below.

After using the above Newton-Rhaphson method we obtain a streaky profile in the fluid. At high Re we find streaks in the streamwise velocity similar to those in Waleffe (1997). However, as we decrease the Reynold's number for constant and large Weissenberg number, we find that the streaks in the streamwise velocity become less pronounced. This can be explained by considering that at low Reynold's number the fluid has a lower inertia, so it is more difficult for the lift up effect to produce streaks in the streamwise velocity.

Although we do not see streaks in the streamwise velocity, we do see them in the first normal stress difference, $N_1 = T_{xx} - T_{yy}$ (figure **??**). These streaks appear in much the same place as the streamwise velocity streaks appear in the Newtonian self-sustaining process. As noted earlier, instabilities in viscoelastic fluids are brought about by large changes in the first normal stress difference, since this brings about polymer stretching of the kind seen in the Weissenberg effect. It is important to note that the purely elastic 1st normal stress difference shows very large gradients near the wall, suggesting that resolving the instability in this base profile will be more difficult than in the Newtonian case.

3. Linear Stability Analysis

Having obtained the full base profile of the problem, we then performed a linear stability analysis, to look for instabilities that might produce waviness in the streaks. These wavy instabilities are responsible for sustaining the exact coherent state in the Newtonian version of the process. This gives us the linear stability equations,

$$(\nabla \mathbf{v})^T + (\nabla \mathbf{v}) = \tau + Wi \left[\frac{\partial \tau}{\partial t} + (\mathbf{V} \cdot \nabla)\tau + (\mathbf{v} \cdot \nabla)T \right. \tag{3.1}$$

$$\left. - (\nabla \mathbf{v})^T \tau - (\nabla \mathbf{v})^T T - \tau(\nabla \mathbf{V}) - T(\nabla \mathbf{v}) \right] \tag{3.2}$$

We decompose the disturbance velocities in the same basis as above (equation 2.2), but include streamwise dependence

$$\check{g}(x, y, z, t) = \sum_{n=-N}^{N} \sum_{m=0}^{M+1} g_{m,n} T_m(y) \mathrm{e}^{i(k_x x + n\gamma z)} \mathrm{e} i\lambda t \tag{3.3}$$

where g can be any of the disturbance variables $(u, v, w, p, \boldsymbol{\tau}_{ij})$. To increase the numerical stability of the problem, we use free slip boundary conditions on the disturbance velocities, $\frac{\partial u}{\partial y}(\pm 1) = v(\pm 1) = \frac{\partial w}{\partial y}(\pm 1) = 0$.

The linearised system of equations now gives an eigenvalue problem for the growth rate of the instability λ at every streamwise wavenumber of the disturbance.

The solution to the eigenvalue problem provides spectra for which eigenmodes with positive growth rates are unstable.

As the Reynold's number is decreased, we find that the base profile becomes more stable. The dispersion relation is reduced in height and moves to lower streamwise wavenumbers. By about $Re = 100$ the base profile has become completely stable. The Newtonian instability is no longer present at this Reynold's number. However, once the Reynolds number becomes negligible in comparison to the Weissenberg number, we begin to see a purely elastic instability arise at very low streamwise wavenumber 2. This purely elastic instability is hugely amplified by further reductions in the Reynold's number.

We can further examine how the purely elastic instability changes with changing Weissenberg number. We find that it grows as the Weissenberg number increases, and saturates by around Wi 20. Doubling the amplitude of the rolls increases the width of the instablity by about a third and the height, 3 fold.

3.1. *Cauchy boundary conditions*

To investigate the affect of free slip boundary conditions on linear stability analysis, we implemented Cauchy boundary conditions,

$$\alpha \left. \frac{\partial u}{\partial y} \right|_{y=\pm 1} + (1 - \alpha) u(y = \pm 1) = 0 \tag{3.4}$$

$$v(y = \pm 1) = 0 \tag{3.5}$$

$$\alpha \left. \frac{\partial w}{\partial y} \right|_{y=\pm 1} + (1 - \alpha) w(y = \pm 1) = 0 \tag{3.6}$$

Where α is a control parameter which controls the relative strength of the free slip to no-slip conditions. (Slip length?)

We found that on decreasing α the instability grows in strength and broadens (figure 4). If we examine the dependence of the instability at one wavenumber, $k_x = 0.01$, it appears that the growth rate of the no-slip system tends to infinity as $\alpha \to 0$ (figure 7).

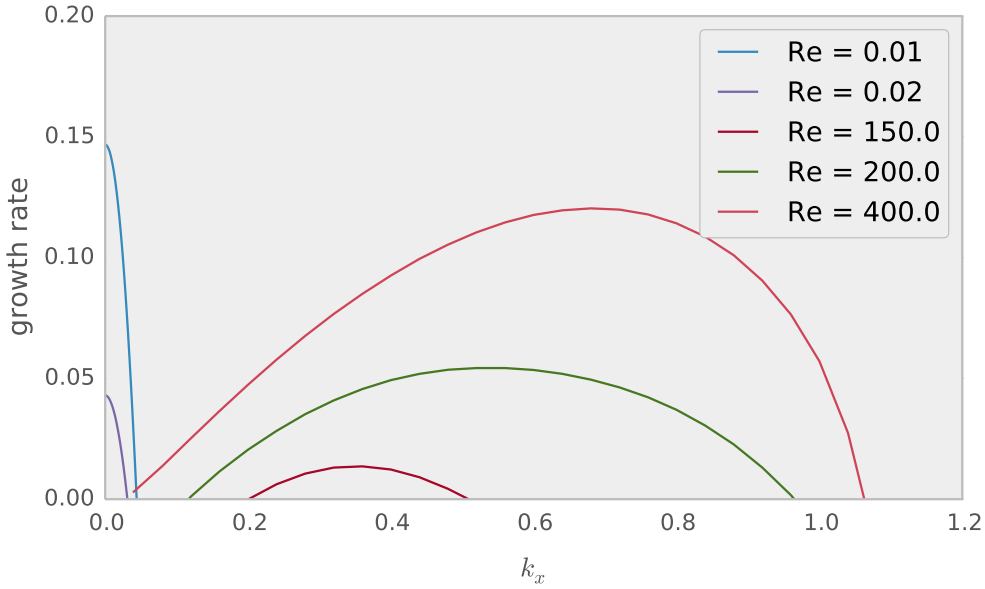

Figure 2: Dispersion relations as the Reynold's number is decreased at $Wi = 2$, $\beta = 0.1$ and amp $= 0.02$. A clear instability can be seen at low k_x in the purely elastic regime.

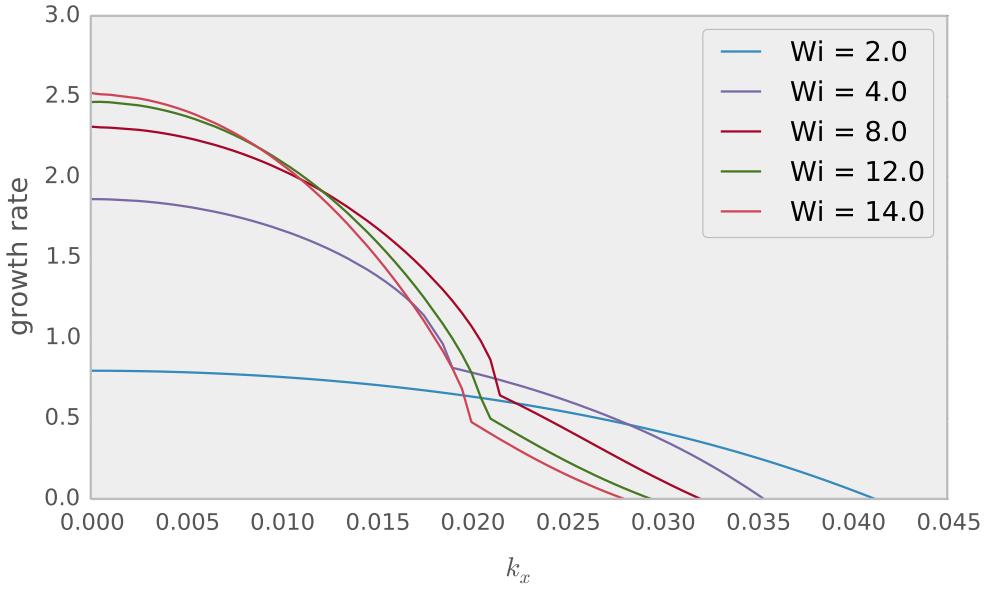

Figure 3: Dispersion relations as the Wi is decreased at $Re = 0.001$, $\beta = 0.1$ and amp $=$ 0.02. The instability grows and then saturates.

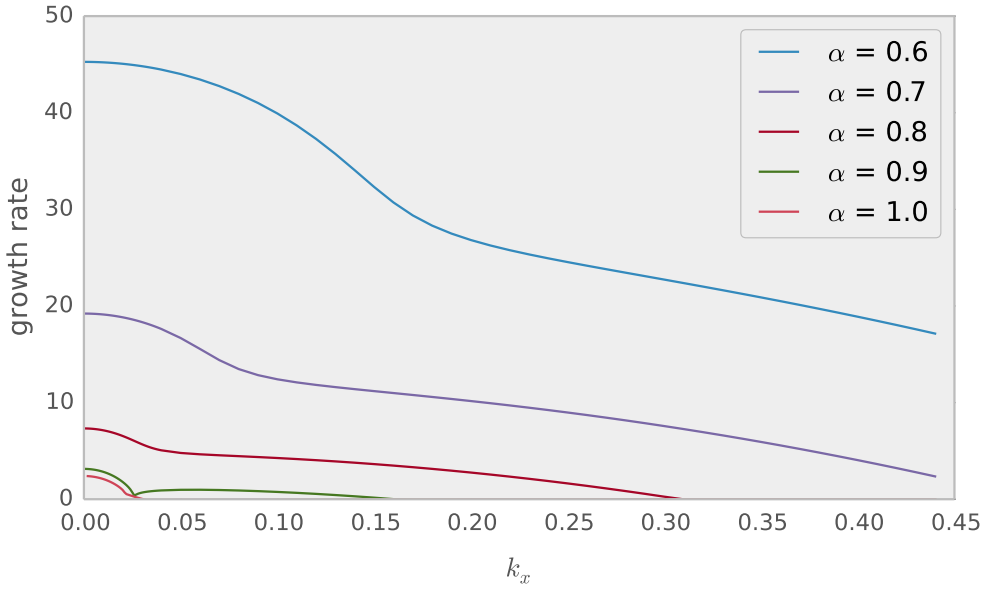

Figure 4: Dispersion relations as α the slip parameter, is reduced. As the system becomes closer to no-slip at the walls the instability grows.

4. Nonlinear feedback on the rolls

In Fabian Waleffe's treatment of the Newtonian version of this self-sustaining process Waleffe (1997), he found that the self-interaction terms due to the eigenvector of the instability give feedback on the original rolls. Although not conclusive, this is good evidence that the cycle might be closed. The eigenvector of the viscoelastic instability is quite different to that of the Newtonian instability. Although the components of the instability are large at the walls, the velocity is less important for the instability of the purely elastic fluid than the first normal stress difference. We find that N_1 is large away from the walls, another encouraging sign for a viscoelastic self-sustaining process (6).

A schematic analysis for the nonlinear feedback similar to that performed by Waleffe Waleffe (1997) requires solving for the rolls due to forcing from the nonlinear terms in the Oldroyd-B equation as well as the Newtonian nonlinear terms,

$$\nabla_2^4 \overline{\Psi}^x = Re\overline{(\mathbf{v}\cdot\nabla)\nabla^2\Psi}^x - (1-\beta)\left(\overline{\frac{\partial^2 T_{yy}}{\partial y \partial z}}^x - \overline{\frac{\partial^2 T_{zz}}{\partial y \partial z}}^x + \overline{\frac{\partial^2 T_{yz}}{\partial z \partial z}}^x - \overline{\frac{\partial^2 T_{yz}}{\partial y \partial y}}^x\right) \tag{4.1}$$

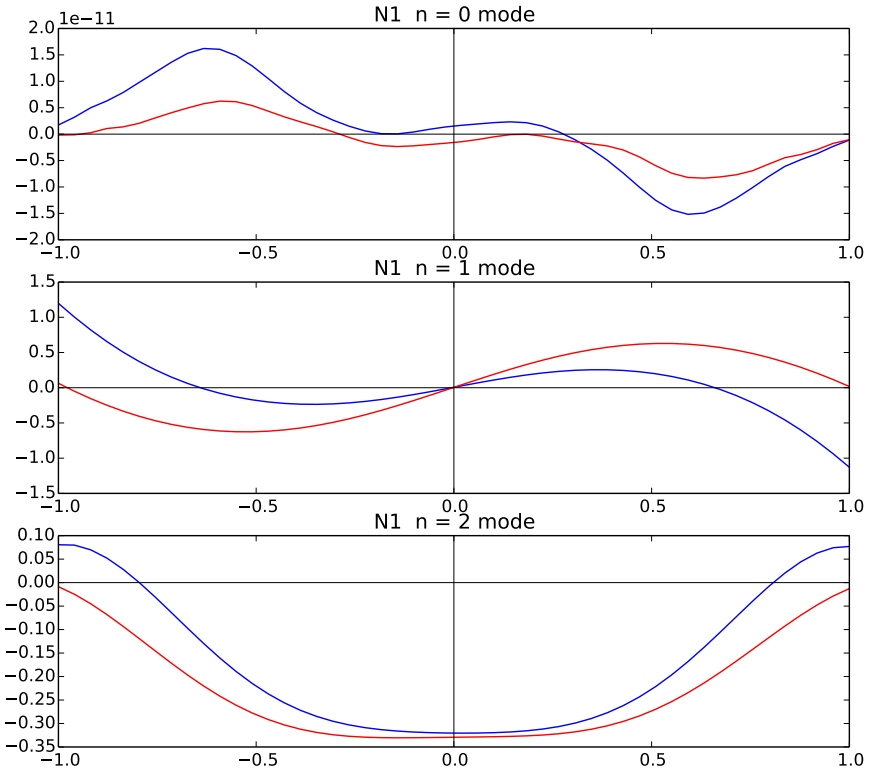

Figure 5: Eigenmodes of the first normal stress difference of the viscoelastic instability at $Wi = 2.0$, $Re = 0.02$, $\beta = 0.1$, amp=0.02 and $k_x = 0.01$.

$$\overline{T_{yz}}^x = Wi\left[-\overline{(\mathbf{v}\cdot\nabla)\tau_{yz}}^x - \overline{\frac{\partial u}{\partial x}\tau_{yz}}^x + \overline{\frac{\partial v}{\partial x}\tau_{xy}}^x\right. \tag{4.2}$$

$$\left. + \overline{\frac{\partial v}{\partial z}\tau_{zz}}^x + \overline{\frac{\partial w}{\partial x}\tau_{xy}}^x + \overline{\frac{\partial w}{\partial y}\tau_{yy}}^x\right] \tag{4.3}$$

$$\overline{T_{yy}}^x = -Wi\overline{(\mathbf{v}\cdot\nabla)\tau_{yy}}^x + 2Wi\left[\overline{\frac{\partial v}{\partial x}\tau_{xy}}^x + \overline{\frac{\partial v}{\partial y}\tau_{yy}}^x + \overline{\frac{\partial v}{\partial z}\tau_{yz}}^x\right] \tag{4.4}$$

$$\overline{T_{zz}}^x = -Wi\overline{(\mathbf{v}\cdot\nabla)\tau_{zz}}^x + 2Wi\left[\overline{\frac{\partial w}{\partial x}\tau_{xz}}^x + \overline{\frac{\partial w}{\partial y}\tau_{yz}}^x + \overline{\frac{\partial w}{\partial z}\tau_{zz}}^x\right] \tag{4.5}$$

$$V = \frac{\partial \Psi}{\partial z} \tag{4.6}$$

Presumably, the no slip instability will have large gradients in the velocities and stresses at the walls as well as those in the bulk. Nevertheless, the shape of the rolls is largly independent of the forcing, and so we don't expect any change to the nonlinear feedback.

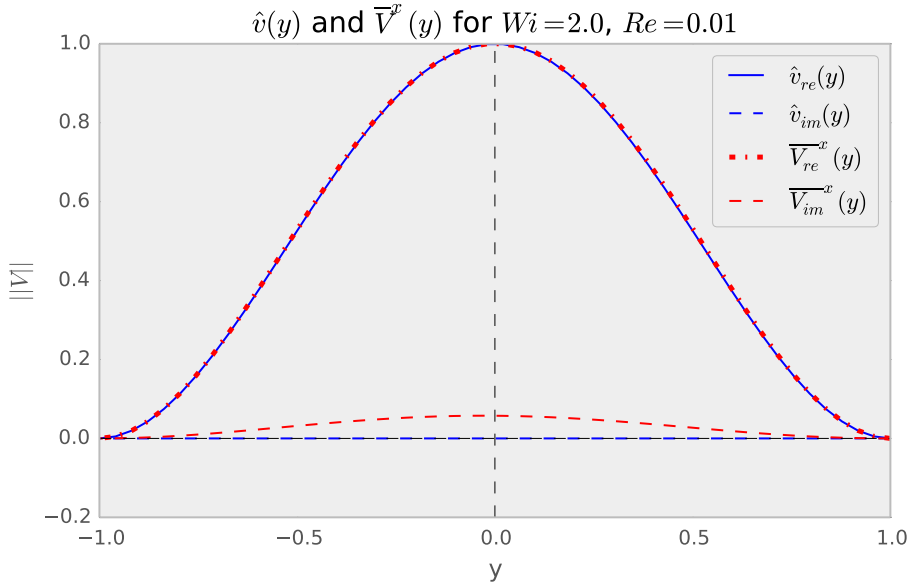

Figure 6: In blue the original amplitude of the rolls in the wall normal direction. Solid line is the real part, dashed is the imaginary part. In red the rolls obtained via nonlinear feedback from the viscoelastic instability at $Wi = 2.0$, $Re = 0.01$, $\beta = 0.1$, amp=0.02 and $k_x = 0.001$. Dot-dashed is the real part and dashed is the imaginary part.

When we completely remove slip at the walls the instability appears infinitely amplified (figure 7). A possible explanation for this is that the instability moves into a region very close to the boundaries as we introduce free slip and can no longer be resolved. It is clear from figure 8 that the first normal stress difference introduced via the instability moves towards the walls as α tends to zero.

5. Discussion and conclusion

We have shown that the velocity profile for the plane Couette viscoelastic self-sustaining process is susceptible to a viscoelastic lift up effect and does become streaky in the purely elastic regime. This streaky base profile is linearly unstable, with a range of wave numbers between about $k_x = 0$ and $k_x = 0.04$. The eigenmodes of this instability are localised in the centre of the channel.

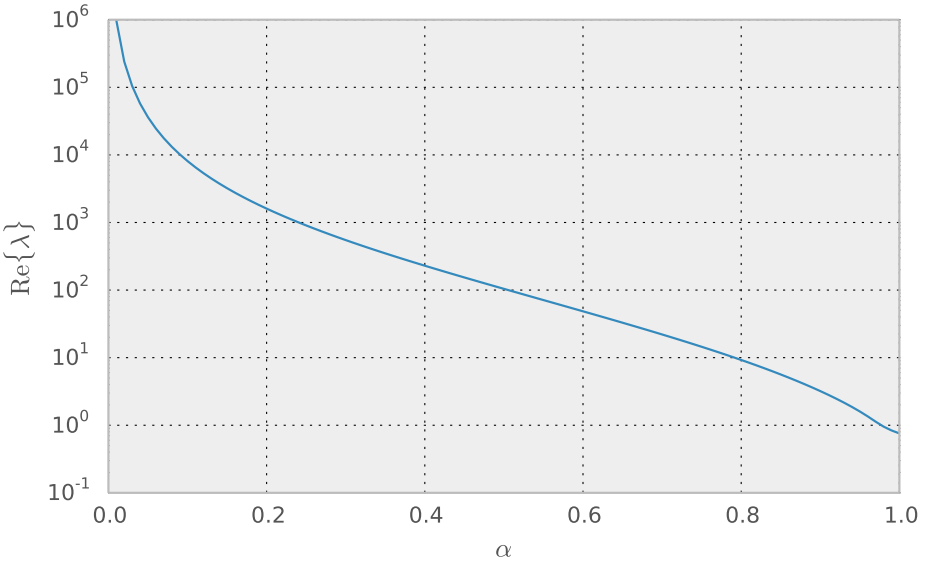

Figure 7: Growth rate of an eigenvalue at $k_x = 0.01$ as α the slip parameter, is reduced. The growth rate assymtotes to the no-slip condition.

REFERENCES

Byars, Jeffrey A., Öztekin, Alparslan, Brown, Robert A. & Mckinley, Gareth H. 1994 Spiral instabilities in the flow of highly elastic fluids between rotating parallel disks. *Journal of Fluid Mechanics* **271**, 173.

Chandler, Gary J. & Kerswell, Rich R. 2013 Invariant recurrent solutions embedded in a turbulent two-dimensional Kolmogorov flow. *Journal of Fluid Mechanics* **722**, 554–595.

Cvitanović, Predrag 2013 Recurrent flows: the clockwork behind turbulence. *Journal of Fluid Mechanics* **726** (1990), 1–4.

Ellingsen, T. & Palm, E. 1975 Stability of linear flow. *Physics of Fluids* **18** (4), 487.

Groisman, A. & Steinberg, V. 2000 Elastic turbulence in a polymer solution flow. *Nature* **405** (6782), 53–5.

Hof, Björn, van Doorne, Casimir W H, Westerweel, Jerry, Nieuwstadt, Frans T M, Faisst, Holger, Eckhardt, Bruno, Wedin, Hakan, Kerswell, Richard R & Waleffe, Fabian 2004 Experimental observation of nonlinear traveling waves in turbulent pipe flow. *Science (New York, N.Y.)* **305** (5690), 1594–8.

Kawahara, Genta & Kida, Shigeo 2001 Periodic motion embedded in plane Couette turbulence: regeneration cycle and burst. *Journal of Fluid Mechanics* **449**, 291.

Kreilos, Tobias & Eckhardt, Bruno 2012 Periodic orbits near onset of chaos in plane Couette flow. *Chaos (Woodbury, N.Y.)* **22** (4), 047505.

Landahl, MT 1980 A note on an algebraic instability of inviscid parallel shear flows. *Journal of Fluid Mechanics* **98**, 243–251.

Larson, R. G., Shaqfeh, Eric S. G. & Muller, S. J. 1990 A purely elastic instability in Taylor Couette flow. *Journal of Fluid Mechanics* **218**, 573.

Morozov, Alexander N. & van Saarloos, Wim 2007 An introductory essay on subcritical instabilities and the transition to turbulence in visco-elastic parallel shear flows. *Physics Reports* **447** (3-6), 112–143.

Pan, L., Morozov, A., Wagner, C. & Arratia, P. E. 2013 Nonlinear Elastic Instability in Channel Flows at Low Reynolds Numbers. *Physical Review Letters* **110** (17), 174502.

Samanta, Devranjan, Dubief, Yves, Holzner, Markus, Schäfer, Christof, Morozov,

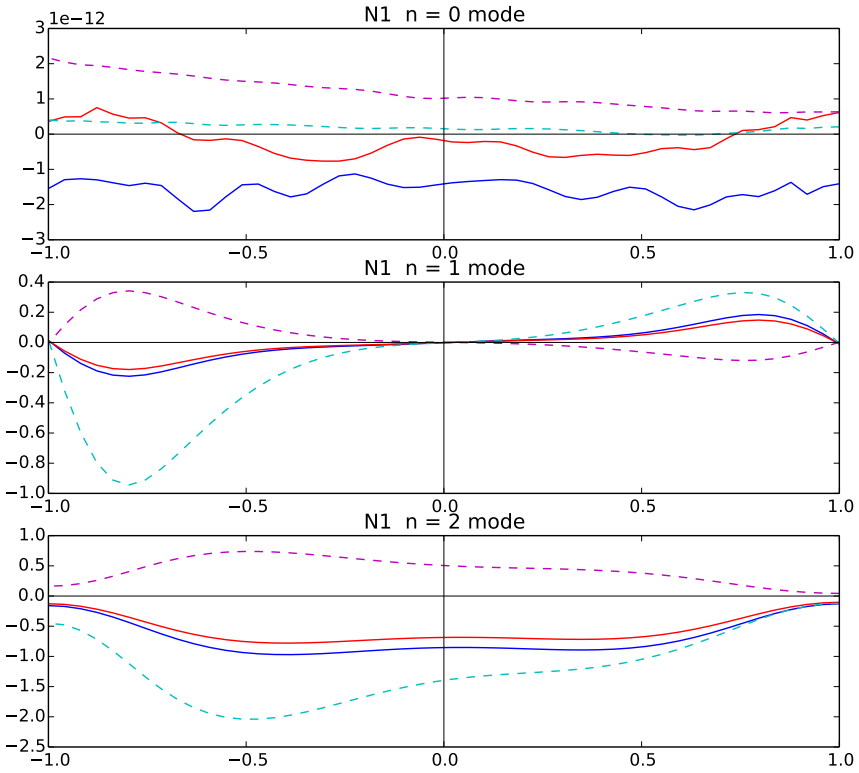

Figure 8: Eigenmodes of the first normal stress difference at $k_x = 0.01$ as α the slip parameter, is reduced. As the slip at the walls is reduced, the first normal stress difference of the instablity becomes more and more localised at the walls.

Alexander N, Wagner, Christian & Hof, Björn 2013 Elasto-inertial turbulence. *Proceedings of the National Academy of Sciences of the United States of America* **110** (26), 10557–62.

Stone, Philip, Waleffe, Fabian & Graham, Michael 2002 Toward a Structural Understanding of Turbulent Drag Reduction: Nonlinear Coherent States in Viscoelastic Shear Flows. *Physical Review Letters* **89** (20), 208301.

Stone, Philip A., Roy, Anshuman, Larson, Ronald G., Waleffe, Fabian & Graham, Michael D. 2004 Polymer drag reduction in exact coherent structures of plane shear flow. *Physics of Fluids* **16** (9), 3470.

Sureshkumar, R., Beris, Antony N. & Handler, Robert A. 1997 Direct numerical simulation of the turbulent channel flow of a polymer solution. *Physics of Fluids* **9** (3), 743.

Waleffe, Fabian 1997 On a self-sustaining process in shear flows. *Physics of Fluids* **9** (4), 883.

Wedin, H & Kerswell, RR 2004 Exact coherent structures in pipe flow: travelling wave solutions. *Journal of Fluid Mechanics* pp. 1–42.

Weissenberg, K 1947 A continuum theory of rheological phenomena. *Nature* .